

# $[\text{Ni}(\text{P}^{\text{Ph}}_2\text{N}^{\text{Bn}}_2)_2(\text{CH}_3\text{CN})]^{2+}$ as an Electrocatalyst for $\text{H}_2$ Production: Dependence on Acid Strength and Isomer Distribution

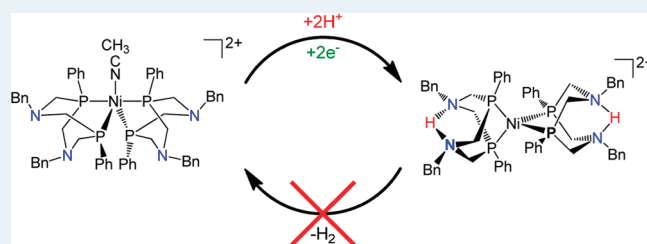
Aaron M. Appel,\* Douglas H. Pool, Molly O'Hagan, Wendy J. Shaw, Jenny Y. Yang, M. Rakowski DuBois, Daniel L. DuBois,\* and R. Morris Bullock

Center for Molecular Electrocatalysis, Pacific Northwest National Laboratory, P.O. Box 999, K2-57, Richland, Washington 99352, United States

Supporting Information

**ABSTRACT:**  $[\text{Ni}(\text{P}^{\text{Ph}}_2\text{N}^{\text{Bn}}_2)_2(\text{CH}_3\text{CN})]^{2+}$  (where  $\text{P}^{\text{Ph}}_2\text{N}^{\text{Bn}}_2$  is 1,5-dibenzyl-3,7-diphenyl-1,5-diaza-3,7-diphosphacyclooctane), has been studied as an electrocatalyst for the production of hydrogen in acetonitrile. Strong acids, such as *p*-cyanoanilinium, protonate  $[\text{Ni}(\text{P}^{\text{Ph}}_2\text{N}^{\text{Bn}}_2)_2(\text{CH}_3\text{CN})]^{2+}$  prior to reduction under catalytic conditions, and an effective  $\text{p}K_{\text{a}}$  of  $6.7 \pm 0.4$  was determined for the protonation product. Through multinuclear NMR spectroscopy studies, the nickel(II) complex was found to be doubly protonated without any observed singly protonated species. In the doubly protonated complex, both protons are positioned exo with respect to the metal center and are stabilized by an N–H–N hydrogen bond. The formation of exo protonated isomers is proposed to limit the rate of hydrogen production because the protons are unable to gain suitable proximity to the reduced metal center to generate  $\text{H}_2$ . Preprotonation of  $[\text{Ni}(\text{P}^{\text{Ph}}_2\text{N}^{\text{Bn}}_2)_2(\text{CH}_3\text{CN})]^{2+}$  has been found to shift the catalytic operating potential to more positive potentials by up to 440 mV, depending upon the conditions. The half-wave potential for the catalytic production of  $\text{H}_2$  depends linearly on the pH of the solution and indicates a proton-coupled electron transfer reaction. The overpotential remains low and nearly constant at  $74 \pm 44$  mV over the pH range of 6.2–11.9. The catalytic rate was found to increase by an order of magnitude by increasing the solution pH or through the addition of water.

**KEYWORDS:** electrocatalysis, catalyst, hydrogen production, pendant amine, PCET, potential



## INTRODUCTION

The need for the energy-efficient production and utilization of fuels or energy carriers such as  $\text{H}_2$  will increase with the utilization of nonfossil energy sources, including solar, wind, and nuclear energy. The production of electricity from many nonfossil energy sources provides motivation for the development of fast and energy-efficient electrocatalysts for the storage of electrical energy in chemical bonds. Platinum is the best catalyst for both the production and utilization of hydrogen, written in eq 1 as the forward and reverse reaction, respectively. However, the limited abundance and therefore the high cost of platinum hinders its widespread use as an electrocatalyst<sup>1</sup> for common applications or in large scale reactions. Inspiration for the use of nonprecious metal catalysts can be found in hydrogenase enzymes, which operate at low overpotentials and with turnover frequencies for  $\text{H}_2$  production and consumption on the order of  $10^3$ – $10^4$   $\text{s}^{-1}$  while utilizing inexpensive metals such as iron and nickel.<sup>2,3</sup>



Electrocatalysts for both hydrogen production and utilization based upon the synthetic molecular complexes  $\text{Ni}(\text{P}^{\text{R}}_2\text{N}^{\text{R}'_2})_2^{2+}$  have been reported (see Scheme 1).<sup>4–9</sup> For  $\text{H}_2$  oxidation catalysts, such as  $\text{Ni}(\text{P}^{\text{Cy}}_2\text{N}^{\text{Bn}}_2)_2^{2+}$  (Cy = cyclohexyl,

Bn = benzyl), reaction with  $\text{H}_2$  (the counterclockwise process in Scheme 1) is thermodynamically favored and forms the doubly nitrogen-protonated nickel(0) complex,  $\text{Ni}(\text{P}^{\text{Cy}}_2\text{N}^{\text{Bn}}_2\text{H})_2^{2+}$ . This is the first spectroscopically observable complex in the catalytic cycle.<sup>5,10</sup> This step is followed by deprotonation, one-electron oxidation, a second deprotonation, and then a second one-electron oxidation to regenerate  $\text{Ni}(\text{P}^{\text{Cy}}_2\text{N}^{\text{Bn}}_2)_2^{2+}$ .

In the absence of an external base, the  $\text{H}_2$  addition product,  $\text{Ni}(\text{P}^{\text{Cy}}_2\text{N}^{\text{Bn}}_2\text{H})_2^{2+}$ , can be observed as three isomers at room temperature, distinguished by the position of the proton in each ligand, either endo or exo with respect to the metal center, as shown in Scheme 2.<sup>5,10</sup> Since  $\text{H}_2$  addition results in double protonation at the amines, these isomers are referred to as endo-endo, endo-exo, and exo-exo to specify the relative location of the two protons. Spectroscopic studies have shown that the endo-endo isomer is the sole product observed from  $\text{H}_2$  addition at  $-70$  °C,<sup>10</sup> but at room temperature, intermolecular proton transfer results in the formation of the

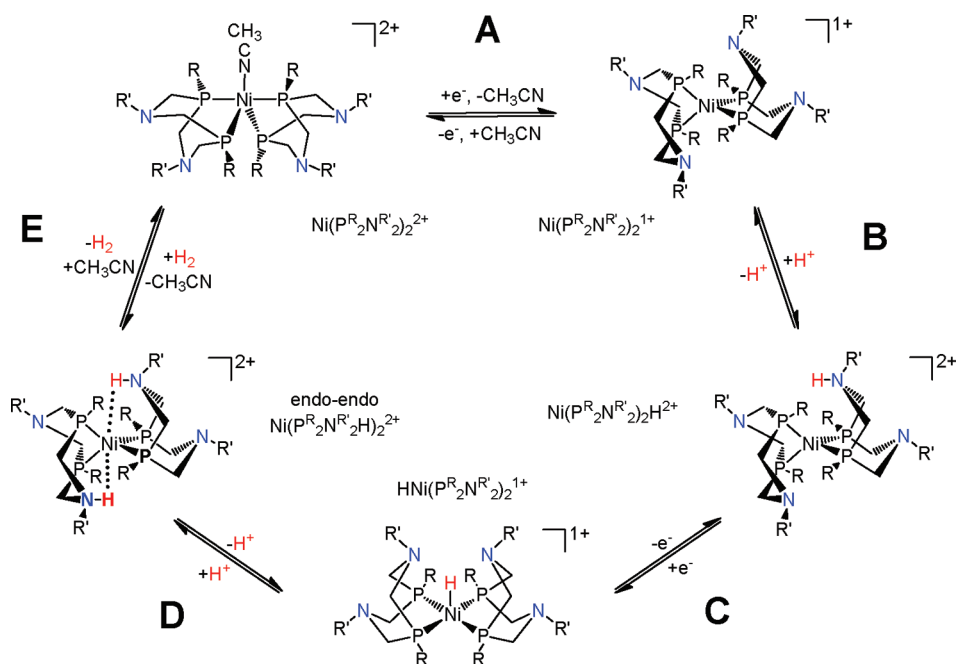
**Special Issue:** Victor S. Y. Lin Memorial Issue

**Received:** February 20, 2011

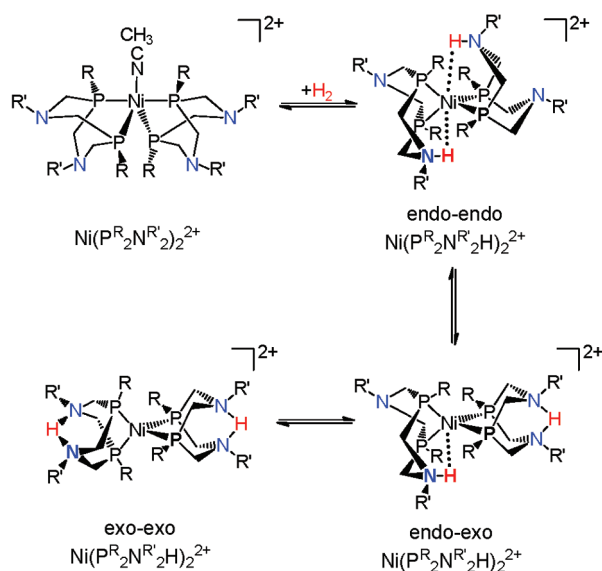
**Revised:** April 7, 2011

**Published:** April 22, 2011

**Scheme 1. Proposed Electrochemical Cycle for H<sub>2</sub> Production (clockwise) or Oxidation (counter clockwise) Using Ni(P<sup>R</sup><sub>2</sub>N<sup>R'</sup><sub>2</sub>)<sub>2</sub><sup>2+</sup> Catalysts**



**Scheme 2. Reaction of Ni(P<sup>R</sup><sub>2</sub>N<sup>R'</sup><sub>2</sub>)<sub>2</sub><sup>2+</sup> with H<sub>2</sub> To Form Ni(P<sup>R</sup><sub>2</sub>N<sup>R'</sup><sub>2</sub>H)<sub>2</sub><sup>2+</sup> As Three Different Isomers, Where Each of the Two Ligands Is Protonated Either Endo or Exo with Respect to the Metal Center**



additional isomers. These isomers can be considered the H<sub>2</sub> addition product of Ni<sup>II</sup>(P<sup>Cy</sup><sub>2</sub>N<sup>Bn</sup><sub>2</sub>)<sub>2</sub><sup>2+</sup> or the double protonation product of Ni<sup>0</sup>(P<sup>Cy</sup><sub>2</sub>N<sup>Bn</sup><sub>2</sub>)<sub>2</sub>.

For H<sub>2</sub> production, the electrocatalytic cycle is thought to proceed as the reverse of the hydrogen oxidation cycle (clockwise rotation in Scheme 1), starting with one-electron reduction

of Ni(P<sup>Ph</sup><sub>2</sub>N<sup>Ph</sup><sub>2</sub>)<sub>2</sub><sup>2+</sup>, protonation, a second one-electron reduction, and then the second protonation. The overall two-electron, two-proton addition is then followed by H<sub>2</sub> elimination, which may include essential isomerization of Ni(P<sup>Ph</sup><sub>2</sub>N<sup>Ph</sup><sub>2</sub>)<sub>2</sub><sup>2+</sup> from exo-exo and endo-exo to endo-endo, as only the latter isomer is expected to be catalytically active by allowing the two protons to gain sufficient proximity to nickel for H<sub>2</sub> formation. For most of the H<sub>2</sub> production catalysts, the diprotonated Ni(0) species have not been observed because H<sub>2</sub> elimination is thermodynamically favored by an estimated 9 kcal/mol for typical catalysts, such as Ni(P<sup>Ph</sup><sub>2</sub>N<sup>Bn</sup><sub>2</sub>)<sub>2</sub><sup>2+</sup>.<sup>11</sup>

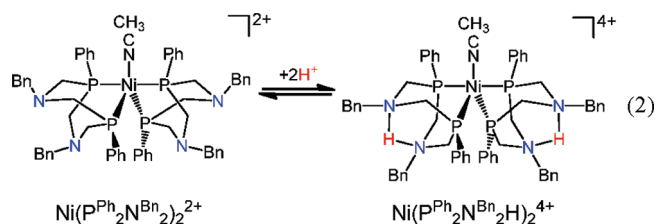
Ni(P<sup>Ph</sup><sub>2</sub>N<sup>Bn</sup><sub>2</sub>)<sub>2</sub><sup>2+</sup> is a H<sub>2</sub> production catalyst with pendant amines that are more basic than those in Ni(P<sup>Ph</sup><sub>2</sub>N<sup>Ph</sup><sub>2</sub>)<sub>2</sub><sup>2+</sup>; as a result, the thermodynamic driving force for H<sub>2</sub> elimination from the diprotonated Ni(0) form is reduced to 2.7 kcal/mol at 25 °C.<sup>8</sup> Ni(P<sup>Ph</sup><sub>2</sub>N<sup>Bn</sup><sub>2</sub>)<sub>2</sub><sup>2+</sup> was measured to have a turnover frequency for H<sub>2</sub> formation that was significantly lower (5 s<sup>-1</sup>) than the analogous catalyst with N-Ph bases, Ni(P<sup>Ph</sup><sub>2</sub>N<sup>Ph</sup><sub>2</sub>)<sub>2</sub><sup>2+</sup> (350 s<sup>-1</sup>), when the systems were studied under similar conditions.<sup>8</sup> Those preliminary studies demonstrated that Ni(P<sup>Ph</sup><sub>2</sub>N<sup>Bn</sup><sub>2</sub>)<sub>2</sub><sup>2+</sup> was reduced at potentials positive of the Ni(II/I) couple of this complex under acidic conditions. This behavior is consistent with either protonation prior to reduction of Ni(II) to Ni(I) or reduction of Ni(II) to Ni(I) followed by a fast protonation reaction. In either case, the protonation reaction influences the potential at which the electron transfer occurs, thereby indicating that the electron and proton transfer reactions are coupled.<sup>12–15</sup> In this paper, we report detailed studies of the protonation of Ni<sup>II</sup>(P<sup>Ph</sup><sub>2</sub>N<sup>Bn</sup><sub>2</sub>)<sub>2</sub><sup>2+</sup> and Ni<sup>0</sup>(P<sup>Ph</sup><sub>2</sub>N<sup>Bn</sup><sub>2</sub>)<sub>2</sub> and how these protonation reactions influence both the catalytic potentials and rates of electrocatalytic production of H<sub>2</sub>. Although catalytic rates for this system are not high, the studies reported here provide unique insights into the mechanism of the more active Ni(P<sup>Ph</sup><sub>2</sub>N<sup>Ph</sup><sub>2</sub>)<sub>2</sub><sup>2+</sup> derivatives.

## RESULTS

**NMR Studies of the Protonation of  $\text{Ni}^{\text{II}}(\text{P}^{\text{Ph}}_2\text{N}^{\text{Bn}}_2)_2^{2+}$  and  $\text{Ni}^{\text{O}}(\text{P}^{\text{Ph}}_2\text{N}^{\text{Bn}}_2)_2$ .** Addition of *p*-cyanoanilinium (1–4 equiv), 2,6-dichloroanilinium (1–2 equiv), or trifluoromethanesulfonic acid (<2 equiv) to  $\text{Ni}(\text{P}^{\text{Ph}}_2\text{N}^{\text{Bn}}_2)_2^{2+}$  resulted in  $^{31}\text{P}\{^1\text{H}\}$  NMR spectra containing a broad singlet at 3.6 ppm for  $\text{Ni}(\text{P}^{\text{Ph}}_2\text{N}^{\text{Bn}}_2)_2^{2+}$  and a new broad singlet at –15.8 ppm. Upon cooling the samples from room temperature to –40 °C, resonances for both the starting  $\text{Ni}(\text{P}^{\text{Ph}}_2\text{N}^{\text{Bn}}_2)_2^{2+}$  and the new species split, as shown in Figure 1.

The similar temperature responses and splitting suggests similar structures and symmetry for  $\text{Ni}(\text{P}^{\text{Ph}}_2\text{N}^{\text{Bn}}_2)_2^{2+}$  and the protonated complex. Under more acidic conditions, the ratio of the new resonance to the starting material increased, but additional decomposition products and side products grew in more rapidly. For comparison with the decomposition products, the free ligand  $\text{P}^{\text{Ph}}_2\text{N}^{\text{Bn}}_2$  was reacted with acid in  $\text{CD}_3\text{CN}$  and yielded the primary peaks observed in the  $^{31}\text{P}$  NMR for the decomposition products, consistent with decomposition by ligand protonation and dissociation (see the Experimental Section for details).

In the  $^1\text{H}$  spectrum, many of the aromatic and  $\text{CH}_2$  resonances of the starting complex overlapped those of the new complex; however, a new peak at 10.4 ppm was observed, which was distinct from any of the resonances for the starting complex (Figure 2, top spectrum). On the basis of previous studies,<sup>10</sup> this singlet was assigned as a N–H resonance. To verify this assignment and determine the number of nitrogen atoms coupled to the proton,  $^{15}\text{N}$ -labeled  $\text{Ni}(\text{P}^{\text{Ph}}_2^{15}\text{N}^{\text{Bn}}_2)_2^{2+}$  was analyzed under the same conditions (Figure 2, bottom spectrum). For the  $^{15}\text{N}$  labeled sample, the resonance at 10.4 ppm was split into a triplet with  $^1J_{\text{NH}} = 34$  Hz, as previously observed for a proton that is “pinched” by the two pendant amines on one ligand and therefore split by two  $^{15}\text{N}$  nuclei.<sup>10</sup> The observation of a triplet for the N–H resonance is consistent with ligand protonation *exo* with respect to the metal, as illustrated in eq 2.



By directly observing the  $^{15}\text{N}$  spectrum, only two peaks were observed for the nickel complexes: one corresponding to  $\text{Ni}(\text{P}^{\text{Ph}}_2\text{N}^{\text{Bn}}_2)_2^{2+}$  (–343.3 ppm) and one new resonance (–334.2 ppm). Using a  $^1\text{H}$ – $^{15}\text{N}$  HSQC experiment, the only  $^1\text{H}$ – $^{15}\text{N}$  correlation observed was between this new  $^{15}\text{N}$  resonance and the 10.4 ppm resonance in the  $^1\text{H}$  NMR spectrum. The spectroscopic data is consistent with forming only one new complex in which all the pendant amines are equivalent and are in the *exo*-protonated form with the two amines on each ligand sharing a proton, as shown in eq 2 for  $\text{Ni}(\text{P}^{\text{Ph}}_2\text{N}^{\text{Bn}}_2\text{H})_2^{4+}$ . In addition, formation of a new, doubly protonated nickel complex is consistent with the stoichiometry observed for products of the reaction; specifically, that for every equivalent of the protonated nickel complex that was formed, 2 equiv of deprotonated base

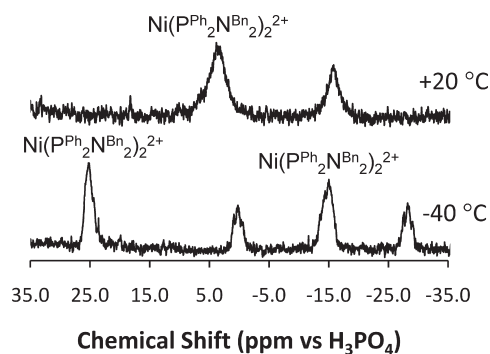


**Figure 1.**  $^{31}\text{P}\{^1\text{H}\}$  NMR spectra of  $\text{Ni}(\text{P}^{\text{Ph}}_2\text{N}^{\text{Bn}}_2)_2^{2+}$  in  $\text{CD}_3\text{CN}$  in the presence of 1 equiv of 2,6-dichloroanilinium at +20 °C (top) and –40 °C (bottom). The resonances for  $\text{Ni}(\text{P}^{\text{Ph}}_2\text{N}^{\text{Bn}}_2)_2^{2+}$  are labeled.

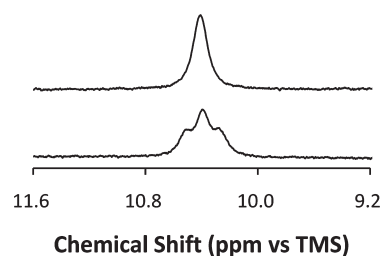
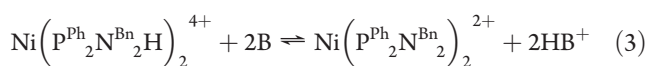


**Figure 2.**  $^1\text{H}$  spectra of  $^{15}\text{N}$  labeled  $\text{Ni}(\text{P}^{\text{Ph}}_2^{15}\text{N}^{\text{Bn}}_2)_2^{2+}$  in the presence of 4 equiv of *p*-cyanoanilinium at +20 °C, decoupled by  $^{15}\text{N}$  (top) and undecoupled (bottom).

were also formed, as measured by  $^{31}\text{P}$  and  $^1\text{H}$  NMR spectroscopy.

The  $\text{pK}_a$  of  $\text{Ni}(\text{P}^{\text{Ph}}_2\text{N}^{\text{Bn}}_2\text{H})_2^{4+}$  in acetonitrile was determined relative to 2,6-dichloroanilinium ( $\text{pK}_a = 5.06$ )<sup>16</sup> and *p*-cyanoanilinium ( $\text{pK}_a = 7.0$ ).<sup>17</sup> Using  $^1\text{H}$  NMR spectroscopy, the aromatic resonances for each substituted anilinium and aniline coalesced into average resonances due to fast exchange. The weighted averages of the chemical shifts for the substituted anilinium and aniline were used to determine the ratio of acid to base for the  $\text{pK}_a$  reference. The analogous ratio for  $\text{Ni}(\text{P}^{\text{Ph}}_2\text{N}^{\text{Bn}}_2\text{H})_2^{4+}$  and  $\text{Ni}(\text{P}^{\text{Ph}}_2\text{N}^{\text{Bn}}_2)_2^{2+}$  was determined from the  $^{31}\text{P}$  NMR spectra, in which the areas of the resonances for the two species were integrated. Using these ratios for the reaction as written in eq 3, the equilibrium constant was determined. Equation 4 was then solved to yield the average  $\text{pK}_a$  of  $6.7 \pm 0.4$  for the two sequential deprotonations of  $\text{Ni}(\text{P}^{\text{Ph}}_2\text{N}^{\text{Bn}}_2\text{H})_2^{4+}$ , although a singly protonated complex was never observed.



$$\text{average } \text{pK}_{a,\text{analyte}} = \text{pK}_{a,\text{ref}} - 0.5 \times \log(K_{\text{eq}}) \quad (4)$$

Reaction of  $\text{Ni}(\text{P}^{\text{Ph}}_2\text{N}^{\text{Bn}}_2)_2^{2+}$  with less than 2 equiv of trifluoromethanesulfonic acid resulted in the formation of a mixture of  $\text{Ni}(\text{P}^{\text{Ph}}_2\text{N}^{\text{Bn}}_2)_2^{2+}$  and  $\text{Ni}(\text{P}^{\text{Ph}}_2\text{N}^{\text{Bn}}_2\text{H})_2^{4+}$ . Addition of water (0.55 M) to this mixture had three primary effects: the N–H resonance in the  $^1\text{H}$  NMR spectrum was no longer observable, consistent with the exchange of the bridging N–H–N proton with water; the two  $^{31}\text{P}$  resonances moved closer together, suggesting chemical exchange on the NMR time scale between  $\text{Ni}(\text{P}^{\text{Ph}}_2\text{N}^{\text{Bn}}_2)_2^{2+}$  and  $\text{Ni}(\text{P}^{\text{Ph}}_2\text{N}^{\text{Bn}}_2\text{H})_2^{4+}$ ; and

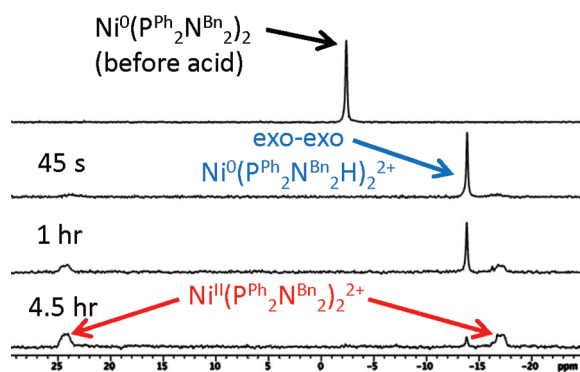


**Figure 3.**  $^{31}\text{P}\{^1\text{H}\}$  NMR spectra of  $\text{Ni}^0(\text{P}^{\text{Ph}}_2\text{N}^{\text{Bn}}_2)_2$  in the presence of 2 equiv of 2,6-dichloroanilinium at  $-53^\circ\text{C}$ .

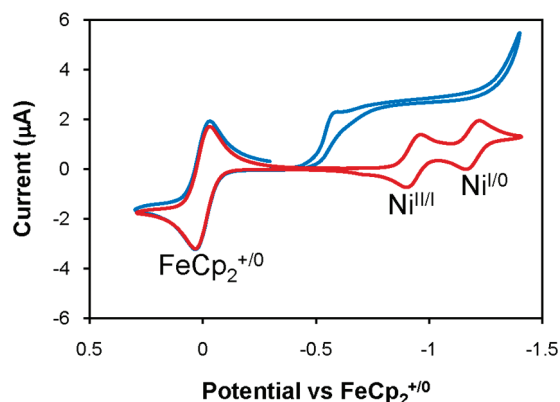


**Figure 4.** Cyclic voltammograms of  $\text{Ni}(\text{P}^{\text{Ph}}_2\text{N}^{\text{Bn}}_2)_2$  (0.7 mM) before addition of acid (red trace) and after addition of *p*-cyanoanilinium (blue trace, 0.12 M). Data collected in acetonitrile with 0.2 M  $\text{NET}_4\text{BF}_4$  using a glassy carbon working electrode with a scan rate of 0.05 V/s.

the ratio of  $\text{Ni}(\text{P}^{\text{Ph}}_2\text{N}^{\text{Bn}}_2)_2^{2+}$  to  $\text{Ni}(\text{P}^{\text{Ph}}_2\text{N}^{\text{Bn}}_2\text{H})_2^{4+}$  increased. The last observation is consistent with water acting as a base in acetonitrile, particularly at a concentration of 0.55 M, wherein the formation of higher hydrates,  $\text{H}_3\text{O}^+ \cdot (\text{H}_2\text{O})_x$ , can influence the effective  $\text{p}K_a$  of hydronium.<sup>18</sup>

Reaction of  $\text{Ni}^0(\text{P}^{\text{Ph}}_2\text{N}^{\text{Bn}}_2)_2$  with 2 equiv of 2,6-dichloroanilinium triflate at  $-53^\circ\text{C}$  in a 1:2 mixture of acetonitrile and THF resulted in the rapid formation of the doubly protonated exo-exo  $\text{Ni}(\text{P}^{\text{Ph}}_2\text{N}^{\text{Bn}}_2\text{H})_2^{2+}$  product, as indicated by  $^{31}\text{P}$  NMR spectroscopy, Figure 3. After 1 h, the sample contained 50% exo-exo, and 50%  $\text{Ni}(\text{P}^{\text{Ph}}_2\text{N}^{\text{Bn}}_2)_2^{2+}$ . After 4.5 h, the sample contained 10% exo-exo and 90%  $\text{Ni}(\text{P}^{\text{Ph}}_2\text{N}^{\text{Bn}}_2)_2^{2+}$ . These data suggest a fast, kinetically controlled protonation of the  $\text{Ni}^0$  complex to form first the exo-exo isomer that undergoes deprotonation and reprotonation to form the endo-endo isomer that rapidly evolves  $\text{H}_2$  and the  $\text{Ni}(\text{P}^{\text{Ph}}_2\text{N}^{\text{Bn}}_2)_2^{2+}$  complex.

**Electrochemical Studies.** Cyclic voltammetry (CV) in acetonitrile was used to investigate  $\text{Ni}(\text{P}^{\text{Ph}}_2\text{N}^{\text{Bn}}_2)_2^{2+}$  as an electrocatalyst for hydrogen production under highly acidic conditions in acetonitrile. In the absence of acid, two reversible one-electron waves are observed at  $-0.94\text{ V}$  for the  $\text{Ni}(\text{II}/\text{I})$  couple and  $-1.19\text{ V}$  for the  $\text{Ni}(\text{I}/\text{O})$  couple, versus the ferrocenium/ferrocene couple in acetonitrile solutions, typical of this class of complexes (Figure 4, red trace). When  $\text{Ni}(\text{P}^{\text{Ph}}_2\text{N}^{\text{Bn}}_2)_2^{2+}$  was reduced in the presence of a strong acid, such as *p*-cyanoanilinium ( $\text{p}K_a^{\text{MeCN}} = 7.0$ ),<sup>17</sup> a new

plateau-shaped wave was observed significantly positive of the  $\text{Ni}(\text{II}/\text{I})$  couple, as illustrated by the blue trace in Figure 4.

The positive shift in potential and corresponding current enhancement was observed using either *p*-cyanoanilinium or protonated DMF (dimethylformamide) as the acid source. The reduction wave was observed as far positive as  $-0.53\text{ V}$  using *p*-cyanoanilinium, or  $-0.50\text{ V}$  using protonated DMF (where the potential is measured at the half-height of the new cathodic wave). To evaluate the electrocatalytic rates for the reduction of protons to dihydrogen, the catalytic current was measured under conditions in which the acid concentration was high enough that the rate was no longer dependent on this concentration. The ratio of this catalytic current ( $i_{\text{cat}}$ ) to the peak current in the absence of acid ( $i_p$ ) was used in eq 5 to determine  $k_{\text{obs}}$ , the first-order catalytic rate constant, or turnover frequency (where  $R$  is the universal gas constant,  $T$  is the temperature in Kelvin,  $F$  is Faraday's constant, and  $v$  is the scan rate).<sup>19–22</sup>

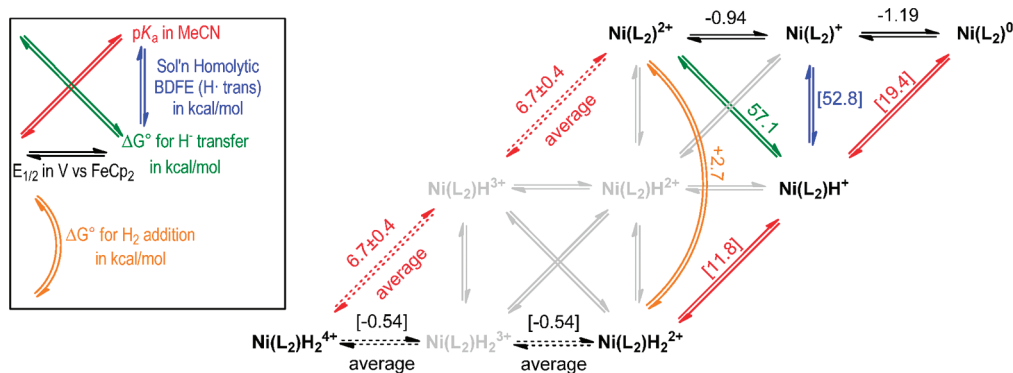
$$\frac{i_{\text{cat}}}{i_p} = \frac{2}{0.446} \sqrt{\frac{RTk_{\text{obs}}}{Fv}} \quad (5)$$

Using *p*-cyanoanilinium tetrafluoroborate, the electrocatalytic turnover frequency was  $<0.5\text{ s}^{-1}$  with 0.12 M acid (due to the low catalytic current enhancement, eq 5 cannot be accurately applied,<sup>19</sup> but will give an upper limit on the rate). A similar rate was observed using protonated DMF as the acid source. For comparison with these results with unbuffered acid solutions, 1:1 buffer solutions of substituted aniliniums and anilines were used to determine reduction potentials and catalytic rates, as shown in Table 1. For the series of conditions shown in Table 1, the reduction potentials (measured at the half-height of the cathodic wave) were observed to linearly track the solution pH, thereby resulting in a nearly constant overpotential<sup>23</sup> of  $74 \pm 44\text{ mV}$  over the pH range of 6.2–11.9.

Addition of water (up to  $\sim 5\text{ M}$ ) to the solutions of catalyst and either buffered or unbuffered acid resulted in a significant increase in current as well as a negative shift in reduction potentials. One example of this is shown in Figure 5 for the system containing 1:1 buffered *p*-cyanoanilinium and *p*-cyanoaniline. For this set of conditions, the reduction potential shifted 150 mV negative from  $-0.61$  to  $-0.76\text{ V}$ , and the observed catalytic rate increased by an order of magnitude upon addition of water, from  $<0.4$  to  $3.6\text{ s}^{-1}$ . Similar increases in rate were observed for all of the acids and bases used, with the exception of buffered *p*-anisidinium/*p*-anisidine. For this specific case, the rate without water was  $3.7\text{ s}^{-1}$ , and any addition of water resulted in lower rates. For a complete list of potentials and rates in the presence of water, see the Supporting Information.

**Thermochemical Studies.** Using a thermochemical cycle starting with the experimentally determined average  $\text{p}K_a$  of  $\text{Ni}(\text{P}^{\text{Ph}}_2\text{N}^{\text{Bn}}_2\text{H})_2^{4+}$  (6.7) and the free energy for addition of  $\text{H}_2$  to  $\text{Ni}(\text{P}^{\text{Ph}}_2\text{N}^{\text{Bn}}_2)_2^{2+}$  ( $+2.7\text{ kcal/mol}$ ),<sup>11</sup> the average reduction potential for  $\text{Ni}(\text{P}^{\text{Ph}}_2\text{N}^{\text{Bn}}_2\text{H})_2^{4+}$  to  $\text{Ni}(\text{P}^{\text{Ph}}_2\text{N}^{\text{Bn}}_2)_2^{2+}$  can be determined to be  $-0.54\text{ V}$  vs  $\text{FeCp}_2^{+/0}$ . This data, in conjunction with the existing thermochemical data for  $\text{Ni}(\text{P}^{\text{Ph}}_2\text{N}^{\text{Bn}}_2)_2^{2+}$ ,<sup>11</sup> can be used to construct the thermochemical diagram in Scheme 3, in which all of the values are free energies in acetonitrile solution (for details, see the Supporting Information). Scheme 3 represents different states in which the  $\text{Ni}(\text{P}^{\text{Ph}}_2\text{N}^{\text{Bn}}_2)_2^{2+}$  complex may exist, most of which have been observed (those in gray have not been observed). Horizontal transitions represent changes in charge; vertical transitions represent changes in the number of

**Scheme 3. Experimental Thermochemical Data for  $\text{Ni}(\text{P}^{\text{Ph}}_2\text{N}^{\text{Bn}}_2)_2^{2+}$  and Related Species in Acetonitrile, Showing the Relationships between  $E_{1/2}$ ,  $\text{p}K_a$ , Homolytic Solution BDFE,  $\Delta G^\circ_{\text{H}^-}$ , and  $\Delta G^\circ_{\text{H}_2}$  Values<sup>a</sup>**



<sup>a</sup> Formulas are intended to indicate only composition, not structure (nickel hydrides vs protonated amines). Values in brackets were determined using the measured values and thermodynamic cycles. Species in gray have not been directly observed. Values over dashed arrows are average values for a multistep process, such as double protonation.

**Table 1. Electrocatalytic Performance of  $\text{Ni}(\text{P}^{\text{Ph}}_2\text{N}^{\text{Bn}}_2)_2^{2+}$  As a Function of pH, in Acetonitrile with 0.2 M  $\text{NET}_4\text{BF}_4$**

acid used (1:1 buffer with conjugate base)	$\text{p}K_a$ in MeCN	catalytic $E_{1/2}$ <sup>a</sup> (V vs $\text{FeCp}_2^{+/0}$ )	overpotential <sup>b</sup> (mV)	rate <sup>c</sup> ( $\text{s}^{-1}$ )
2,5-dichloranilinium	6.21	-0.58	73	<0.4
<i>p</i> -cyanoanilinium	7.0	-0.61	54	<0.4
<i>p</i> - $\text{CF}_3$ -anilinium	8.03	-0.72	105	<0.4
<i>p</i> -bromoanilinium	9.43	-0.79	92	<0.8
anilinium	10.62	-0.84	72	<0.9
<i>p</i> -anisidinium	11.86	-0.89	48	3.7

<sup>a</sup> Potential at half-height vs  $\text{FeCp}_2^{+/0}$ , as measured by CV. <sup>b</sup> Difference between observed potential and theoretical  $\text{H}_2$  electrode potential in MeCN at the solution pH.<sup>23</sup> <sup>c</sup> Maximum catalytic rate observed in the acid-concentration-independent region. Rates <1.6  $\text{s}^{-1}$  are estimates because eq 5 does not apply at the low corresponding current enhancement.<sup>19</sup>

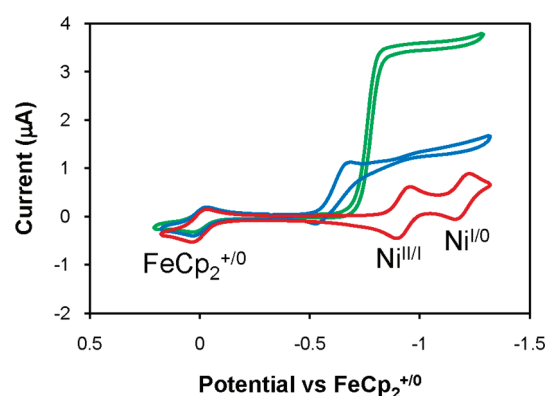


**Figure 5.** Cyclic voltammograms of  $\text{Ni}(\text{P}^{\text{Ph}}_2\text{N}^{\text{Bn}}_2)_2^{2+}$  (0.6 mM) before addition of acid (red trace), in the presence of a 1:1 solution of *p*-cyanoanilinium and *p*-cyanoaniline (0.036 M total, blue trace), and after addition of water to the buffered solution (4.6 M  $\text{H}_2\text{O}$  total, green trace). Data collected in acetonitrile with 0.2 M  $\text{NET}_4\text{BF}_4$  using a glassy carbon working electrode with a scan rate of 0.05 V/s.

hydrogen atoms (expressed as solution bond dissociation free energies, BDFEs, in MeCN). Diagonal transitions represent

combinations of vertical and horizontal transitions: either  $\text{p}K_a$  values ( $\text{H}^\cdot - \text{e}^-$ ) or free energies for  $\text{H}^-$  cleavage ( $\text{H}^\cdot + \text{e}^-$ ). It should be noted that the charge and number of hydrogen atoms is intended to specify only composition, not structure, meaning that  $\text{Ni}(\text{L}_2)\text{H}^+$  could be either a nickel(II) hydride or a nickel(0) species that is protonated at nitrogen. In addition, the nickel(II) species in many cases have a coordinated acetonitrile, but this is not explicitly shown in the scheme. Scheme 3 can be used to determine the thermodynamic driving force of each step shown in Scheme 1 as well as the energetics of alternate pathways, such as those involving  $\text{Ni}(\text{P}^{\text{Ph}}_2\text{N}^{\text{Bn}}_2\text{H})_2^{4+}$  that would be expected for this catalyst under highly acidic conditions.

## DISCUSSION

The fastest catalysts for  $\text{H}_2$  production in the series of  $\text{Ni}(\text{P}^{\text{R}}_2\text{N}^{\text{R}'}_2)_2^{2+}$  derivatives contain aromatic groups on the pendant amines, and introduction of electron-withdrawing groups on the arene further enhances the turnover frequencies.<sup>24</sup> In contrast, the complex containing the more basic benzyl group on the pendant amines in  $\text{Ni}(\text{P}^{\text{Ph}}_2\text{N}^{\text{Bn}}_2)_2^{2+}$  catalyzes  $\text{H}_2$  formation at significantly slower rates, but with lower overpotentials. This observation is consistent with the proposal<sup>24</sup> that increased basicity disfavors the elimination of  $\text{H}_2$  from the doubly protonated  $\text{Ni}(0)$  species in Scheme 1. The slower rate of  $\text{H}_2$  production in this catalyst and the increased basicity of the pendant amine provide an opportunity to gain a better understanding of how proton and electron transfer reactions are coupled in this class of catalysts and how the site of protonation of the pendant amine influences catalytic rates.

**Coupling of Proton and Electron Transfer Steps.** One role of the pendant amines in the catalytic oxidation and production of  $\text{H}_2$  by  $\text{Ni}(\text{P}^{\text{R}}_2\text{N}^{\text{R}'}_2)_2^{2+}$  complexes is to serve as proton relays, assisting the transfer of protons between the solution and the metal site. This process involves two steps: an intermolecular transfer of a proton between an acid or base in solution and the N atom of a pendant amine, and an intramolecular step involving the transfer of a proton between the N atom and the metal. Both of these steps can be coupled to electron transfer reactions. Studies of  $\text{H}_2$  oxidation catalysts such as  $\text{Ni}(\text{P}^{\text{Cy}}_2\text{N}^{\text{Bn}}_2)_2^{2+}$  indicate that oxidation of the  $\text{HNi}(\text{P}^{\text{Cy}}_2\text{N}^{\text{Bn}}_2)_2^+$  intermediate occurs at a potential that is 0.6–0.8 V more negative than those

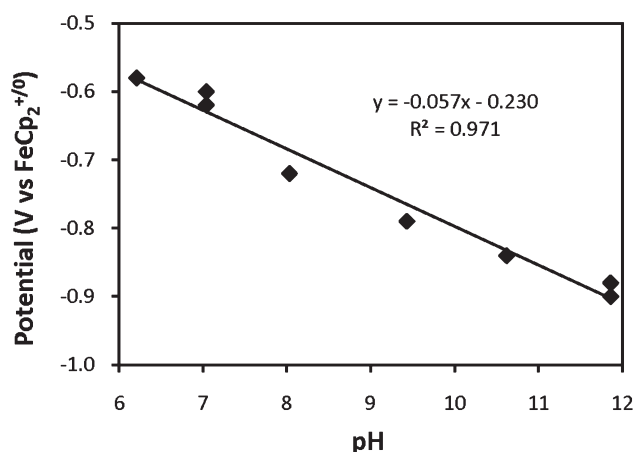


**Figure 6.** Potential vs solution pH for  $\text{Ni}(\text{P}^{\text{Ph}}_2\text{N}^{\text{Bn}}_2)_2^{2+}$  using a series of pH buffered solutions in MeCN.

observed for analogous  $[\text{HNi}(\text{diphosphine})_2]^+$  complexes without the proton relays.<sup>6,25</sup> These large shifts in potential have been attributed to coupling of the electron transfer step with the intramolecular transfer of a proton from Ni to N, as shown in step C of Scheme 1. It is also likely that the intermolecular proton transfer steps B and D of Scheme 1 can couple with the electron transfer steps A and C. This coupling of intermolecular proton transfer with electron transfer is one focus of this study.

Previous electrocatalysts for hydrogen production based upon the  $\text{Ni}(\text{P}^{\text{Ph}}_2\text{N}^{\text{C}_6\text{H}_4\text{X}}_2)_2^{2+}$  platform exhibit electrocatalytic current enhancement at or close to the Ni(II/I) couple,<sup>4,10,24</sup> suggesting reduction prior to protonation. For  $\text{Ni}(\text{P}^{\text{Ph}}_2\text{N}^{\text{Bn}}_2)_2^{2+}$ , the catalytic potential was found to be shifted modestly positive of the Ni(II/I) couple when *p*-bromoanilinium ( $\text{p}K_{\text{a}} = 9.43$  in MeCN)<sup>16</sup> was used as the acid.<sup>11</sup> In the present studies, using stronger acids, including *p*-cyanoanilinium ( $\text{p}K_{\text{a}} = 7.0$ )<sup>17</sup> or protonated DMF ( $\text{p}K_{\text{a}} = 6.1$ ),<sup>26</sup> resulted in a substantial positive shift for the reduction potential, as shown in Figure 4. Using *p*-cyanoanilinium, the reduction potential was as much as 410 mV positive of the Ni(II/I) couple in the absence of acid. These results indicate that the intermolecular proton transfer and electron transfer are coupled in that protonation facilitates electron transfer.

When the addition of excess *p*-cyanoanilinium to  $\text{Ni}(\text{P}^{\text{Ph}}_2\text{N}^{\text{Bn}}_2)_2^{2+}$  in dry acetonitrile was monitored by cyclic voltammetry, the resulting wave at  $-0.53$  V appeared to indicate catalysis, on the basis of the wave shape, the current reached a plateau rather than decaying in the usual diffusional manner observed for noncatalytic cyclic voltammograms. The current enhancement ( $i_{\text{cat}}/i_{\text{p}} = 2.3$  at 50 mV/s) was inadequate to provide accurate rates from the comparison of the catalytic current,  $i_{\text{cat}}$ , to the peak current in the absence of acid,  $i_{\text{p}}$ ,<sup>19</sup> but can provide an upper limit for the catalytic rate of  $<0.5$  s<sup>-1</sup>. This slow catalytic rate affects the reversibility of the observed wave, but the potential of the catalytic wave is determined by protonation of the catalyst in either its oxidized or reduced forms. To confirm that the observed potential is controlled by protonation, experiments were carried out to study the effect of solution pH on the catalytic potential. Cyclic voltammetry experiments were carried out over a range of pH values by using 1:1 solutions of the anilinium salts shown in Table 1 and their corresponding

conjugate bases to buffer the solution at a specific pH. Although the complex is a catalyst for H<sub>2</sub> production under these conditions, the slow catalytic rate ensures that a well-defined solution pH can be maintained at the electrode surface through buffering. The results of these experiments are summarized in Table 1 and illustrated in Figure 6.

The half-wave potentials for these buffered solutions shift by 57 mV/pH unit, as shown by the line in Figure 6. The linear tracking of these potentials with the solution pH confirms that the proton and electron transfer steps are coupled, and the observed 57 mV/pH unit is within experimental uncertainty of the 59.2 mV/pH unit that would be expected for a coupled one-proton, one-electron or a two-proton, two-electron process. For strong acids, such as 2,5-dichloroanilinium, protonated DMF, and *p*-cyanoanilinium, diprotonation of the  $\text{Ni}(\text{P}^{\text{Ph}}_2\text{N}^{\text{Bn}}_2\text{H})_2^{2+}$  complex to form  $\text{Ni}(\text{P}^{\text{Ph}}_2\text{N}^{\text{Bn}}_2\text{H})_2^{4+}$  precedes the electron transfer steps. For weaker acids, such as anilinium and *p*-anisidinium,  $\text{Ni}(\text{P}^{\text{Ph}}_2\text{N}^{\text{Bn}}_2)_2^{2+}$  is the dominant species in solution, and reduction of Ni(II) to Ni(I) or Ni(0) likely precedes protonation. In these cases, the potential shifts may be due to a kinetic effect in which electron transfer is followed by a rapid protonation reaction. A third possibility is that the proton transfer and electron transfer reactions are concerted. Regardless of the precise mechanism, which may vary with pH, the coupling of the intermolecular proton transfer and electron transfer steps results in positive shifts of the observed reduction potential as large as 440 mV.

Similar shifts in potential with pH have been reported by Artero, et al.<sup>27</sup> for cobalt diimine-dioxime catalysts containing a proton bridging two oxo groups in close proximity to the metal center. For these cobalt complexes, the catalytic wave is observed to shift 190 mV negative in moving from *p*-cyanoanilinium to anilinium as the acid source ( $\Delta\text{p}K_{\text{a}} = 3.4$  pH units), consistent with the results of the present work and the expectation of a 59.2 mV/pH slope.

**Dependence of the Catalytic Rates on the Site of Protonation.** Additions of *p*-cyanoanilinium tetrafluoroborate to  $\text{Ni}(\text{P}^{\text{Ph}}_2\text{N}^{\text{Bn}}_2)_2^{2+}$  and to the <sup>15</sup>N-labeled analogue were studied by a combination of <sup>1</sup>H, <sup>31</sup>P, and <sup>15</sup>N NMR spectroscopies. A single product was observed to be in equilibrium with the starting compound upon addition of 1–4 equiv of acid, and the product was identified as the doubly exo-protonated, tetracationic species  $\text{Ni}(\text{P}^{\text{Ph}}_2\text{N}^{\text{Bn}}_2\text{H})_2^{4+}$  shown in eq 2. The same products were observed when the stronger acid trifluoromethanesulfonic acid was added. No singly protonated intermediate species was observed in these studies, suggesting that the first protonation does not decrease the driving force for the second, but rather, that the second protonation is easier than the first. The source of this cooperative effect is unclear, but may be the result of steric influences arising from protonation-induced conformational changes.

These NMR studies of  $\text{Ni}(\text{P}^{\text{Ph}}_2\text{N}^{\text{Bn}}_2\text{H})_2^{4+}$  clearly indicate that protonation of  $\text{Ni}(\text{P}^{\text{Ph}}_2\text{N}^{\text{Bn}}_2)_2^{2+}$  occurs at the exo positions of the  $\text{P}^{\text{Ph}}_2\text{N}^{\text{Bn}}_2$  ligand to give the structure shown in eq 2. Similarly, protonation of the Ni(0) species  $\text{Ni}^0(\text{P}^{\text{Ph}}_2\text{N}^{\text{Bn}}_2)_2$  using 2,6-dichloroanilinium at  $-53$  °C in a 1:2 mixture of CD<sub>3</sub>CN and THF resulted initially in the formation of exo-exo  $\text{Ni}(\text{P}^{\text{Ph}}_2\text{N}^{\text{Bn}}_2\text{H})_2^{2+}$  and a small amount of  $\text{Ni}(\text{P}^{\text{Ph}}_2\text{N}^{\text{Bn}}_2)_2^{2+}$ , as determined by <sup>31</sup>P NMR spectroscopy (see Figure 3). Over a period of 4 h, the initially formed exo-exo  $\text{Ni}(\text{P}^{\text{Ph}}_2\text{N}^{\text{Bn}}_2\text{H})_2^{2+}$  converted to  $\text{Ni}(\text{P}^{\text{Ph}}_2\text{N}^{\text{Bn}}_2)_2^{2+}$  with formation of H<sub>2</sub>. These observations are consistent with the slow isomerization of exo-exo  $\text{Ni}(\text{P}^{\text{Ph}}_2\text{N}^{\text{Bn}}_2\text{H})_2^{2+}$  at  $-53$  °C to form the endo-endo

$\text{Ni}(\text{P}^{\text{Ph}}_2\text{N}^{\text{Bn}}_2\text{H})_2^{2+}$  isomer, which eliminates  $\text{H}_2$ , as shown in step E of Scheme 1. Given that the kinetic protonation product is the exo-exo isomer and that isomerization to form the endo-endo isomer is slow, with no build up of the latter intermediate, the observed slow electrocatalytic rates arise from the small fraction of the complex that forms the catalytically active isomer.

These spectroscopic observations are consistent with our electrochemical studies. The very slow rate of catalysis ( $<0.4 \text{ s}^{-1}$ , Table 1) observed when 2,5-dichloroanilinium or *p*-cyanoanilinium were used as acids suggests that the exo-exo isomer of the diprotonated Ni(II) catalyst is maintained upon reduction to the Ni(0) intermediate. The absence of a low-energy pathway for conversion to the catalytically active endo-endo isomer under these conditions accounts for the slow rate of  $\text{H}_2$  formation. For acids such as *p*-bromoanilinium ( $\text{p}K_{\text{a}} = 9.43$ ) and anilinium ( $\text{p}K_{\text{a}} = 10.62$ ) that have much higher  $\text{p}K_{\text{a}}$  values,  $\text{Ni}(\text{P}^{\text{Ph}}_2\text{N}^{\text{Bn}}_2)_2^{2+}$  is not expected to be protonated to any significant extent in solution. However, on the basis of the NMR experiments described in the preceding paragraph, after reduction to Ni(0), protonation would be expected to occur to form exo-exo  $\text{Ni}(\text{P}^{\text{Ph}}_2\text{N}^{\text{Bn}}_2\text{H})_2^{2+}$  ( $\text{p}K_{\text{a}} = 11.8$ ). As a result, the catalytic rates observed under these conditions are also very slow,  $<0.9 \text{ s}^{-1}$ . Only for *p*-anisidinium is a significantly higher rate of catalysis observed. A 1:1 buffer solution of this acid and its conjugate base has a pH of 11.86, which is closely matched to the  $\text{p}K_{\text{a}}$  of  $\text{Ni}(\text{P}^{\text{Ph}}_2\text{N}^{\text{Bn}}_2\text{H})_2^{2+}$  (11.8)<sup>11</sup> and permits deprotonation and reprotonation of this complex. This process facilitates the rate of conversion of the catalytically inactive exo-exo isomer to the catalytically active endo-endo isomer. It is the ability of *p*-anisidine to facilitate the more rapid interconversion of  $\text{Ni}(\text{P}^{\text{Ph}}_2\text{N}^{\text{Bn}}_2\text{H})_2^{2+}$  isomers that produces the unexpected increase in the rate of catalytic hydrogen production as the acidity of the solution decreases.

Upon addition of water (4.4 M) to an unbuffered solution of *p*-cyanoanilinium and  $\text{Ni}(\text{P}^{\text{Ph}}_2\text{N}^{\text{Bn}}_2)_2^{2+}$ , the catalytic rate was found to increase substantially (from an estimated  $<0.5 \text{ s}^{-1}$  to nearly  $8 \text{ s}^{-1}$ ) while the potential shifted negative from a value of  $-0.53$  to  $-0.68 \text{ V}$ , still 260 mV positive of the Ni(II/I) couple in the absence of acid. The negative potential shift suggests that water is acting as a base to deprotonate some of the  $\text{Ni}(\text{P}^{\text{Ph}}_2\text{N}^{\text{Bn}}_2\text{H})_2^{4+}$  species, shifting the effective pH of the solutions by  $\sim 2.5$  pH units (150 mV divided by 59.2 mV/pH unit). Although the  $\text{p}K_{\text{a}}$  of  $\text{H}_3\text{O}^+$  in acetonitrile has been determined to be 2.2, suggesting that  $\text{H}_2\text{O}$  is an inadequate base to deprotonate  $\text{Ni}(\text{P}^{\text{Ph}}_2\text{N}^{\text{Bn}}_2\text{H})_2^{4+}$ , the formation of higher hydrates ( $\text{H}_3\text{O}^+ \cdot (\text{H}_2\text{O})_x$ ) is expected to increase the effective basicity of  $\text{H}_2\text{O}$  in acetonitrile.<sup>18</sup> In addition, solvation of the anilinium ions by water may decrease the acidity of the anilinium ions. Regardless of the mechanism, NMR studies that monitored the ratio of  $\text{Ni}(\text{P}^{\text{Ph}}_2\text{N}^{\text{Bn}}_2)_2^{2+}$  and  $\text{Ni}(\text{P}^{\text{Ph}}_2\text{N}^{\text{Bn}}_2\text{H})_2^{4+}$  in acetonitrile- $d_3$  solutions containing trifluoromethanesulfonic acid confirmed that  $\text{Ni}(\text{P}^{\text{Ph}}_2\text{N}^{\text{Bn}}_2\text{H})_2^{4+}$  is partially deprotonated upon the addition of water and consistent with the negative potential shifts. The addition of water to dry, buffered solutions of the catalyst also results in a substantial increase in the catalytic rate from  $<0.9 \text{ s}^{-1}$  to  $\sim 4\text{--}8 \text{ s}^{-1}$  (see Table S1 of Supporting Information for details) for all acids except anisidinium. These results again suggest that water acts as a base, enhancing the rate of conversion of the exo-exo isomer to the endo-endo isomer and greatly enhancing the electrocatalytic rate for hydrogen production using  $\text{Ni}(\text{P}^{\text{Ph}}_2\text{N}^{\text{Bn}}_2)_2^{2+}$ . Similar rate enhancement with water addition has been recently reported for other  $\text{Ni}(\text{P}^{\text{Ph}}_2\text{N}^{\text{C}_6\text{H}_4\text{X}}_2)_2^{2+}$  catalysts.<sup>24</sup> The decrease in activity observed upon addition of water when

the *p*-anisidinium/*p*-anisidine buffer was used as the acid source is likely due to an increase in the pH of this solution to effective pH values greater than 11.86, the  $\text{p}K_{\text{a}}$  of anisidinium in acetonitrile. In these higher pH solutions, the reduction and protonation steps that convert  $\text{Ni}(\text{P}^{\text{Ph}}_2\text{N}^{\text{Bn}}_2)_2^{2+}$  to  $\text{Ni}(\text{P}^{\text{Ph}}_2\text{N}^{\text{Bn}}_2\text{H})_2^{2+}$  are expected to be thermodynamically unfavorable because  $\text{Ni}(\text{P}^{\text{Ph}}_2\text{N}^{\text{Bn}}_2\text{H})_2^{2+}$  has a  $\text{p}K_{\text{a}}$  of 11.8.

One result of the electrocatalytic potential tracking the solution pH is that the overpotential remains at an average of  $74 \pm 44 \text{ mV}$  across the entire pH range (see Table 1). The deviations are likely due to either experimental error or a discrepancy in the solution pH relative to the  $\text{p}K_{\text{a}}$  due to nonideality, including such effects as homoconjugation. An initial assumption might be that the hydrogen production rates would also not change substantially over this pH range, since the overpotential is remaining essentially constant. However, because the exo-exo to endo-endo conversion rate is enhanced at higher pH values, the hydrogen production rates show the unusual trend of an increase from  $<0.4 \text{ s}^{-1}$  at a pH of 8 or less to  $\sim 3.7 \text{ s}^{-1}$  at pH 11.86 (*p*-anisidinium/*p*-anisidine). For the system reported by Artero, et al,<sup>27</sup> a similar trend is observed for the current enhancement,  $i_{\text{cat}}/i_{\text{p}}$ ; specifically, that for *p*-cyanoanilinium vs anilinium, the weaker acid results in greater current enhancement in cyclic voltammetry experiments.

## SUMMARY AND CONCLUSIONS

Under strongly acidic conditions,  $\text{Ni}(\text{P}^{\text{Ph}}_2\text{N}^{\text{Bn}}_2)_2^{2+}$  is protonated to form an exo-exo doubly protonated complex  $\text{Ni}(\text{P}^{\text{Ph}}_2\text{N}^{\text{Bn}}_2\text{H})_2^{4+}$ . The half-wave potential of the doubly protonated complex is shifted by up to  $+0.44 \text{ V}$  compared with the potential of the Ni(II/I) couple of the unprotonated complex. In fact, the half-wave potential for this catalyst was found to track linearly with solution pH with a slope of 57 mV/pH unit, consistent with the expected 59.2 mV/pH unit shift expected for either a one-proton, one-electron or a two-proton, two-electron coupled process. These results clearly demonstrate that the pendant base is capable of coupling electron transfer processes with intermolecular proton transfer processes as well as the previously observed coupling of the intramolecular proton transfer process. The pendant bases in these complexes can facilitate both intra- and intermolecular proton-coupled electron transfer processes during the catalytic cycle.

The catalytic rate was found to increase with increasing pH or by the addition of water. The increase in turnover frequency is attributed to an increase in the rate of interconversion of exo-protonated and endo-protonated isomers, as promoted by water or the conjugate base of the acid used. Similar rate enhancements due to water addition are observed for the related derivatives,  $\text{Ni}(\text{P}^{\text{Ph}}_2\text{N}^{\text{C}_6\text{H}_4\text{X}}_2)_2^{2+}$ , suggesting that the catalytic rates reported for these complexes may actually be limited by the formation of catalytically inactive exo-protonated species. Studies are in progress to develop catalysts that either avoid exo-protonation or that facilitate more rapid interconversion between exo and endo isomers.

## EXPERIMENTAL PROCEDURES

**Instrumentation.**  $^1\text{H}$  and  $^{31}\text{P}$  NMR spectra were recorded on Varian spectrometers (300 or 500 MHz for  $^1\text{H}$ ) at 22 °C unless otherwise noted. All  $^1\text{H}$  chemical shifts have been internally calibrated to the residual solvent protons.<sup>28</sup> The  $^{31}\text{P}$  NMR spectra were referenced to external phosphoric acid. The  $^{15}\text{N}$  NMR spectra

were referenced to the natural abundance CD<sub>3</sub>CN peak as  $-137$  ppm vs nitromethane.<sup>29</sup> Electrochemical data were collected using a CH Instruments 600 or 1100 series computer-aided three-electrode potentiostat in acetonitrile with 0.2 M tetraethylammonium tetrafluoroborate. For cyclic voltammetry, the working electrode was a glassy carbon disk, the counter electrode was a glassy carbon rod, and a silver-chloride-coated silver wire was used as a pseudoreference electrode and was separated from the main compartment by a Vycor disk (1/8 in. diameter). Ferrocene was used as an internal reference, with all potentials reported versus the FeCp<sub>2</sub><sup>+0</sup> couple.

**Materials.** Reagents were purchased commercially and used without further purification unless otherwise specified. Acetonitrile was dried by activated alumina column in an Innovative Technology, Inc., PureSolv system. CD<sub>3</sub>CN was dried over activated sieves, degassed, and stored in a glovebox. All reactions, syntheses, and manipulations of Ni(P<sup>Ph</sup><sub>2</sub>N<sup>Bn</sup><sub>2</sub>)<sub>2</sub><sup>2+</sup> and its precursors were carried out under nitrogen using standard Schlenk techniques or in a glovebox. Ni(P<sup>Ph</sup><sub>2</sub>N<sup>Bn</sup><sub>2</sub>)<sub>2</sub><sup>2+</sup> was prepared as previously reported,<sup>11</sup> with the <sup>15</sup>N-labeled complex prepared analogously using the <sup>15</sup>N-labeled ligand.<sup>30</sup> 2,6-Dichloroaniline and *p*-cyanoaniline were purified by vacuum sublimation prior to use. *p*-Cyanoanilinium tetrafluoroborate was isolated from *p*-cyanoaniline and tetrafluoroboric acid in ether as previously described.<sup>31</sup> A similar procedure was used for 2,6-dichloroanilinium triflate from the corresponding aniline and triflic acid. The triflate salt of protonated DMF (DMFH<sup>+</sup>OTf<sup>-</sup>) was prepared by the method of Favier and Duñach.<sup>32</sup>

**Electrocatalytic Proton Reduction.** Cyclic voltammetry was used to evaluate the catalytic activity of Ni(P<sup>Ph</sup><sub>2</sub>N<sup>Bn</sup><sub>2</sub>)<sub>2</sub><sup>2+</sup> for proton reduction (as previously described)<sup>19–22</sup> using multiple acids under different conditions. In a typical experiment, a solution of approximately 1 mM ferrocene (internal reference) and 0.5–1.0 mM Ni(P<sup>Ph</sup><sub>2</sub>N<sup>Bn</sup><sub>2</sub>)<sub>2</sub><sup>2+</sup> was used. After an initial CV, sequential additions of an acid solution were made. After each acid addition, a CV was collected. Once the current enhancement reached a maximum, water was added incrementally until the current enhancement no longer increased. See Table 1 for rates and potentials under dry conditions and the Supporting Information for a complete list, including acid/base concentrations, water concentrations, rates, and potentials. It should be noted that for current enhancements ( $i_{\text{cat}}/i_{\text{p}} < 4$  at 50 mV/s (TOF < 1.6 s<sup>-1</sup>),<sup>19</sup> eq 5 is not accurate, but can be used to calculate an upper limit on the rate.

**Protonation of Ni(P<sup>Ph</sup><sub>2</sub>N<sup>Bn</sup><sub>2</sub>)<sub>2</sub><sup>2+</sup>.** In one experiment, 58  $\mu\text{L}$  of 15.4 mg *p*-cyanoanilinium tetrafluoroborate in 0.50 mL CD<sub>3</sub>CN ( $8.7 \times 10^{-3}$  mmol acid) was added to a solution of Ni(P<sup>Ph</sup><sub>2</sub>N<sup>Bn</sup><sub>2</sub>)<sub>2</sub><sup>2+</sup> (10.8 mg,  $8.7 \times 10^{-3}$  mmol) in 0.50 mL CD<sub>3</sub>CN. <sup>1</sup>H and <sup>31</sup>P{<sup>1</sup>H} spectra were collected before and after the addition. After addition of acid, the <sup>1</sup>H NMR spectrum showed a new broad singlet at 10.4 ppm, with the remainder of the spectrum (aromatic and methylene resonances) similar to and convoluted with the resonances from the starting material.<sup>11</sup> The <sup>31</sup>P{<sup>1</sup>H} NMR spectrum showed the initial peak at 3.6 ppm (br, s) and a new peak at  $-15.8$  ppm (br, s). The <sup>31</sup>P{<sup>1</sup>H} NMR spectrum at  $-40$  °C resolved the broad singlets of both species, yielding two broad multiplets for each: 24.6 and  $-15.6$  ppm for the starting material and  $-0.3$  and  $-28.9$  ppm for the new species. The samples were followed with time, up to 10 days. Side products were observed to grow in without appreciable effect upon the measured acid–base equilibrium. These include protonated free ligand (as identified below) at  $-39.4$ ,  $-51.8$ , and

$-65.5$  ppm as well as multiple unidentified singlets from  $+32$  to  $+22$  ppm. Higher acid concentrations or use of stronger acids (2,6-dichloroanilinium or trifluoromethanesulfonic acid) resulted in faster and more extensive formation of side products. Under very acidic conditions, a transient sharp singlet was initially observed at  $-15.4$  ppm, and the intensity of this resonance would decrease with time. After 10 days, addition of excess triethylamine immediately converted most (>80%) of the products back to the starting Ni(P<sup>Ph</sup><sub>2</sub>N<sup>Bn</sup><sub>2</sub>)<sub>2</sub><sup>2+</sup> complex.

**Protonation of Labeled Ni(P<sup>Ph</sup><sub>2</sub><sup>15</sup>N<sup>Bn</sup><sub>2</sub>)<sub>2</sub><sup>2+</sup>.** A sample was prepared with 29.3 mg (0.0234 mmol) of Ni(P<sup>Ph</sup><sub>2</sub><sup>15</sup>N<sup>Bn</sup><sub>2</sub>)<sub>2</sub><sup>2+</sup> and 19.3 mg (0.0937 mmol) of *p*-cyanoanilinium tetrafluoroborate in 0.6 mL of CD<sub>3</sub>CN. The <sup>31</sup>P NMR spectrum displayed the same features as the natural abundance sample, whereas the broad singlet at 10.4 ppm in the <sup>1</sup>H NMR spectrum was split into a broad triplet in the <sup>15</sup>N-labeled sample, with  $J_{\text{NH}} = 34$  Hz. The <sup>15</sup>N spectrum showed three resonances: two resonances for the analytes as well as the natural abundance <sup>15</sup>N peak from the CD<sub>3</sub>CN (used as an internal reference where  $\delta$  is  $-137$  ppm versus nitromethane).<sup>29</sup> One analyte resonance ( $-343.3$  ppm) corresponded to the chemical shift of the starting material, and the other resonance ( $-334.2$  ppm) was assigned as the protonated species. Using the same sample, a <sup>1</sup>H–<sup>15</sup>N HSQC was run. Only one resonance was observed, and it correlated the  $-334.2$  ppm resonance in the <sup>15</sup>N spectrum and the 10.4 ppm resonance in the <sup>1</sup>H spectrum.

**Protonation of the P<sup>Ph</sup><sub>2</sub>N<sup>Bn</sup><sub>2</sub> ligand.** The free P<sup>Ph</sup><sub>2</sub>N<sup>Bn</sup><sub>2</sub> ligand was treated with 2,6-dichloroanilinium triflate ( $pK_{\text{a}}$  in MeCN is 5.06)<sup>16</sup> to determine the <sup>31</sup>P{<sup>1</sup>H} chemical shifts of the products for comparison with the above NMR results. In one experiment, 10.4 mg (0.0216 mmol) of P<sup>Ph</sup><sub>2</sub>N<sup>Bn</sup><sub>2</sub> ligand was combined with 0.27 mL of a 0.21 M solution (0.057 mmol) of 2,6-dichloroanilinium in CD<sub>3</sub>CN. Both <sup>1</sup>H and <sup>31</sup>P{<sup>1</sup>H} NMR spectra were collected, resulting in new unassigned resonances at  $-39.4$ ,  $-51.8$ , and  $-65.5$  ppm in the <sup>31</sup>P{<sup>1</sup>H} NMR spectrum, with ratios of 0.93 to 1.00 to 0.27, respectively. These resonances are consistent with the primary side products observed in the above experiments for the protonation of Ni(P<sup>Ph</sup><sub>2</sub>N<sup>Bn</sup><sub>2</sub>)<sub>2</sub><sup>2+</sup>.

**Water Addition to Protonated Ni(P<sup>Ph</sup><sub>2</sub>N<sup>Bn</sup><sub>2</sub>)<sub>2</sub><sup>2+</sup>.** To a solution of 13.3 mg (0.0107 mmol) Ni(P<sup>Ph</sup><sub>2</sub>N<sup>Bn</sup><sub>2</sub>)<sub>2</sub><sup>2+</sup> in 0.60 mL of CD<sub>3</sub>CN, 1.6  $\mu\text{L}$  (0.018 mmol) trifluoromethanesulfonic acid was added. <sup>1</sup>H and <sup>31</sup>P{<sup>1</sup>H} NMR spectra were collected, with results similar to those observed using *p*-cyanoanilinium, as above. Addition of 6.0  $\mu\text{L}$  deionized, degassed water resulted in a decrease in protonated complex and increase in deprotonated complex. Along with the shift in acid–base equilibria, the line width increased for the deprotonated and protonated resonances in the <sup>31</sup>P spectrum, and the difference in chemical shift between the two resonances decreased from 19.4 ppm to 17.2 ppm. In addition, the N–H resonance at 10.4 ppm in the <sup>1</sup>H spectrum (protonated Ni(P<sup>Ph</sup><sub>2</sub>N<sup>Bn</sup><sub>2</sub>)<sub>2</sub><sup>2+</sup>) was no longer observable.

**$pK_{\text{a}}$  Determination.** The  $pK_{\text{a}}$  values for the protonated aniline derivatives were taken from the self-consistent scale published by Kaljurand, et al.<sup>16</sup> The  $pK_{\text{a}}$  value of 6.1 for protonated DMF was taken from Izutsu.<sup>26</sup> The average  $pK_{\text{a}}$  value for Ni(P<sup>Ph</sup><sub>2</sub>N<sup>Bn</sup><sub>2</sub>)<sub>2</sub><sup>4+</sup> was determined against known bases using <sup>1</sup>H NMR at analyte and reference concentrations <60 mM. The observed acid–base equilibria using the aniline derivatives and Ni(P<sup>Ph</sup><sub>2</sub>N<sup>Bn</sup><sub>2</sub>)<sub>2</sub><sup>2+</sup> gave average <sup>1</sup>H peaks resulting from rapid exchange of protons between the base and acid forms of the reference. For the aniline derivatives, the weighted averages of the shifts were used to determine the ratio of acid to base for each species. The protonated and



deprotonated  $\text{Ni}(\text{P}^{\text{Ph}}_2\text{N}^{\text{Bn}}_2)_2^{2+}$  complex gave separate  $^{31}\text{P}\{^1\text{H}\}$  peaks that were integrated. The ratios of protonated to deprotonated reference and analyte were used to determine the equilibrium constant for eq 3 and, thereafter, the  $\text{p}K_{\text{a}}$  of the analyte in eq 4. The extent of deprotonation of the reference and the extent of protonation of  $\text{Ni}(\text{P}^{\text{Ph}}_2\text{N}^{\text{Bn}}_2)_2^{2+}$  based on the stoichiometry and the above ratios are consistent with double protonation of  $\text{Ni}(\text{P}^{\text{Ph}}_2\text{N}^{\text{Bn}}_2)_2^{2+}$ . The determined average  $\text{p}K_{\text{a}}$  value ( $6.7 \pm 0.4$ ) for the double deprotonation is the average of eight measurements from four independent samples and includes verifications of reversibility. The listed error is twice the standard deviation for all of the values for the eight measurements.

**Synthesis of  $\text{Ni}^0(\text{P}^{\text{Ph}}_2\text{N}^{\text{Bn}}_2)_2$ .** The ligand  $\text{P}^{\text{Ph}}_2\text{N}^{\text{Bn}}_2$  (0.26 g,  $5.5 \times 10^{-4}$  mol) was slurried in THF and cooled to  $-78$  °C. Bis(cyclooctadiene)nickel,  $\text{Ni}(\text{COD})_2$ , (0.077 g,  $2.8 \times 10^{-4}$  mol) was added as a solid under a  $\text{N}_2$  purge. The reaction was stirred at  $-78$  ° for 30 min, then warmed to room temperature and stirred for 1 h. The color changed to yellow, then orange at RT. The solvent was removed under vacuum, and the solid was washed with two 5 mL portions of acetonitrile and dried under vacuum. Yield: 0.197 g, 69%.  $^1\text{H}$  NMR (toluene- $d_8$ ): 2.85 (8 H, d,  $J = 11.5$  Hz,  $\text{CH}_2$ ); 3.34 (8 H, d,  $J = 10.3$  Hz,  $\text{CH}_2$ ); 3.69 (8 H, s,  $\text{PhCH}_2$ ); 7.0–7.2 (m, 32 H, Ph); 7.75 (br s, 8 H, Ph).  $^{31}\text{P}\{^1\text{H}\}$  NMR (toluene- $d_8$ ): 1.48 (s). Anal. Calcd. for  $\text{C}_{60}\text{H}_{64}\text{N}_4\text{P}_4\text{Ni}$ : C, 70.39; H, 6.30; N, 5.47. Found: C, 69.97; H, 6.34; N, 5.29.

**Low-Temperature Protonation of  $\text{Ni}^0(\text{P}^{\text{Ph}}_2\text{N}^{\text{Bn}}_2)_2$ .** A solution of  $\text{Ni}^0(\text{P}^{\text{Ph}}_2\text{N}^{\text{Bn}}_2)_2$  (7 mM) in a 1:2 mixture of  $\text{CD}_3\text{CN}$  and protic THF was cooled to  $-53$  °C and analyzed by  $^{31}\text{P}\{^1\text{H}\}$  NMR spectroscopy. Two equivalents of 2,6-dichloroanilinium triflate were added to the solution, and the sample was reanalyzed  $\sim 45$  s after addition. Data were collected in an array every 60 s over  $\sim 4.5$  h. Assignments for the endo-endo, endo-exo, and exo-exo isomers as well as the  $\text{Ni}(\text{P}^{\text{Ph}}_2\text{N}^{\text{Bn}}_2)_2^{2+}$  were made on the basis of the high-pressure NMR experiments previously described<sup>11</sup> for the addition of  $\text{H}_2$  to  $\text{Ni}(\text{P}^{\text{Ph}}_2\text{N}^{\text{Bn}}_2)_2^{2+}$ .

## ■ ASSOCIATED CONTENT

**Supporting Information.** Examples of the thermochemical cycles used to construct Scheme 3 and a complete copy of Table 1, including rates and potentials in the presences of water. This material is available free of charge via the Internet at <http://pubs.acs.org>.

## ■ AUTHOR INFORMATION

### Corresponding Author

\*E-mails: [aaron.appel@pnl.gov](mailto:aaron.appel@pnl.gov); [daniel.dubois@pnl.gov](mailto:daniel.dubois@pnl.gov).

### Author Contributions

This paper is dedicated to the memory of Victor Lin, in appreciation of his many contributions to chemistry and catalysis.

## ■ ACKNOWLEDGMENT

The authors thank Dr. Herman Cho for helpful discussions about 2D NMR data. This research was supported as part of the Center for Molecular Electrocatalysis, an Energy Frontier Research Center funded by the U.S. Department of Energy, Office of Science, Office of Basic Energy Sciences. Pacific

Northwest National Laboratory is operated by Battelle for the U.S. Department of Energy.

## ■ REFERENCES

- (1) Rakowski DuBois, M.; DuBois, D. L. In *Catalysis Without Precious Metals*; Bullock, R. M., Ed.; Wiley-VCH: Weinheim, 2010; pp 165–180.
- (2) Fontecilla-Camps, J. C.; Volbeda, A.; Cavazza, C.; Nicolet, Y. *Chem. Rev.* **2007**, *107*, 4273–4303.
- (3) Frey, M. *ChemBioChem* **2002**, *3*, 153–160.
- (4) Wilson, A. D.; Newell, R. H.; McNevin, M. J.; Muckerman, J. T.; Rakowski DuBois, M.; DuBois, D. L. *J. Am. Chem. Soc.* **2006**, *128*, 358–366.
- (5) Rakowski DuBois, M.; DuBois, D. L. *C.R. Chim.* **2008**, *11*, 805–817.
- (6) Rakowski DuBois, M.; DuBois, D. L. *Chem. Soc. Rev.* **2009**, *38*, 62–72.
- (7) Rakowski DuBois, M.; DuBois, D. L. *Acc. Chem. Res.* **2009**, *42*, 1974–1982.
- (8) Yang, J. Y.; Bullock, R. M.; Rakowski DuBois, M.; DuBois, D. L. *MRS Bull.* **2011**, *36*, 39–47.
- (9) DuBois, D. L.; Bullock, R. M. *Eur. J. Inorg. Chem.* **2011**, 1017–1027.
- (10) Wilson, A. D.; Shoemaker, R. K.; Miedaner, A.; Muckerman, J. T.; DuBois, D. L.; Rakowski DuBois, M. *Proc. Natl. Acad. Sci.* **2007**, *104*, 6951–6956.
- (11) Frazee, K.; Wilson, A. D.; Appel, A. M.; Rakowski DuBois, M.; DuBois, D. L. *Organometallics* **2007**, *26*, 3918–3924.
- (12) Mayer, J. M. *Annu. Rev. Phys. Chem.* **2004**, *55*, 363–390.
- (13) Huynh, M. H. V.; Meyer, T. J. *Chem. Rev.* **2007**, *107*, 5004–5064.
- (14) Hammes-Schiffer, S. *Acc. Chem. Res.* **2009**, *42*, 1881–1889.
- (15) Chang, C. J.; Chang, M. C. Y.; Damrauer, N. H.; Nocera, D. G. *Biochem. Biophys. Acta* **2004**, *1655*, 13–28.
- (16) Kaljurand, I.; Kutt, A.; Soovali, L.; Rodima, T.; Maemets, V.; Leito, I.; Koppel, I. A. *J. Org. Chem.* **2005**, *70*, 1019–1028.
- (17) Appel, A. M.; Lee, S.-J.; Franz, J. A.; DuBois, D. L.; Rakowski DuBois, M.; Twamley, B. *Organometallics* **2009**, *28*, 749–754.
- (18) Chantooni, M. K.; Kolthoff, I. M. *J. Am. Chem. Soc.* **1970**, *92*, 2236–2239.
- (19) Nicholson, R. S.; Shain, I. *Anal. Chem.* **1964**, *36*, 706–723.
- (20) Saveant, J. M.; Vianello, E. *Electrochim. Acta* **1965**, *10*, 905–920.
- (21) Savéant, J. M.; Vianello, E. *Electrochim. Acta* **1967**, *12*, 629–646.
- (22) Pool, D. H.; DuBois, D. L. *J. Organomet. Chem.* **2009**, *694*, 2858–2865.
- (23) Felton, G. A. N.; Glass, R. S.; Lichtenberger, D. L.; Evans, D. H. *Inorg. Chem.* **2006**, *45*, 9181–9184.
- (24) Kilgore, U. J.; Roberts, J. A. S.; Pool, D. H.; Appel, A. M.; Stewart, M. P.; Rakowski DuBois, M.; Dougherty, W. G.; Kassel, W. S.; Bullock, R. M.; DuBois, D. L. *J. Am. Chem. Soc.* **2011**, *133*, 5861–5872.
- (25) Curtis, C. J.; Miedaner, A.; Ciancanelli, R.; Ellis, W. W.; Noll, B. C.; Rakowski DuBois, M.; DuBois, D. L. *Inorg. Chem.* **2003**, *42*, 216–227.
- (26) Izutsu, K., *Acid–Base Dissociation Constants in Dipolar Aprotic Solvents*; Blackwell Scientific Publications: Oxford, 1990.
- (27) Jacques, P.-A.; Artero, V.; Pécaut, J.; Fontecave, M. *Proc. Natl. Acad. Sci.* **2009**, *106*, 20627–20632.
- (28) Fulmer, G. R.; Miller, A. J. M.; Sherden, N. H.; Gottlieb, H. E.; Nudelman, A.; Stoltz, B. M.; Bercaw, J. E.; Goldberg, K. I. *Organometallics* **2010**, *29*, 2176–2179.
- (29) Duncan, T. M. *Principal Components of Chemical Shift Tensors: A Compilation*, 2nd ed.; The Farragut Press: Madison, WI, 1997.
- (30) Yang, J. Y.; Bullock, R. M.; Shaw, W. J.; Twamley, B.; Frazee, K.; Rakowski DuBois, M.; DuBois, D. L. *J. Am. Chem. Soc.* **2009**, *131*, 5935–5945.
- (31) Appel, A. M.; DuBois, D. L.; Rakowski DuBois, M. *J. Am. Chem. Soc.* **2005**, *127*, 12717–12726.
- (32) Favier, I.; Duñach, E. *Tetrahedron Lett.* **2004**, *45*, 3393–3395.